GA–A24817

IFE TARGET INJECTION TRACKING AND POSITION PREDICTION UPDATE

by
R.W. PETZOLDT and K. JONESTRASK

NOVEMBER 2004

DISCLAIMER

GA–A24817

IFE TARGET INJECTION TRACKING AND POSITION PREDICTION UPDATE

by
R.W. PETZOLDT and K. JONESTRASK

This is a preprint of a paper presented at the 16th ANS Topical Meeting on the Technology of Fusion Energy, Madison, Wisconsin, September 14–16, 2004 and to be published in *Fusion Science and Technology.*

Work supported by
the U.S. Department of Energy
under NRL Subcontract N00173-02-C-6010

GENERAL ATOMICS PROJECT 30183
NOVEMBER 2004

IFE TARGET INJECTION TRACKING AND POSITION PREDICTION UPDATE

Ronald W. Petzoldt and Kevin Jonestrask

General Atomics, PO Box 85608, San Diego, Califoirnia 92186, email: Ronald.Petzoldt@gat.com

To achieve high gain in an inertial fusion energy power plant, driver beams must hit direct drive targets with ±20 μm accuracy (±100 μm for indirect drive). Targets will have to be tracked with even greater accuracy. The conceptual design for our tracking system, which predicts target arrival position and timing based on position measurements outside of the reaction chamber was previously described.[1] *The system has been built and has begun tracking targets at the first detector station. Additional detector stations are being modified for increased field of view. After three tracking stations are operational, position predictions at the final station will be compared to position measurements at that station as a measure of target position prediction accuracy.*

The as-installed design will be described together with initial target tracking and position prediction accuracy results. Design modifications that allow for improved accuracy and/or in-chamber target tracking will also be presented.

I. INTRODUCTION

The fuel [typically Deuterium-Tritium (DT)] for an inertial fusion energy (IFE) power plant is frozen to the inner surface of a small spherical capsule.[2] Driver beams symmetrically hit a direct drive target, causing ablation of the outer surface and compression of the inner fuel. Driver beams heat an enclosed volume within indirect drive targets, producing x-rays that cause ablation of the spherical capsule inside and subsequent fuel compression.

The target injection system must deliver several targets each second to the center of a power plant reaction chamber. The target trajectory must be precisely tracked to provide target position information. The driver beams can then be timed and steered to hit the target with sufficient accuracy.

II. REQUIREMENTS AND ASSUMPTIONS

Target injection and tracking requirements have been determined with input from the IFE community.[3] Driver beams must hit direct drive targets with ±20 μm accuracy and indirect drive targets with ±100 μm accuracy. Because of greater accuracy requirements for direct drive, we have emphasized direct drive target tracking in this design. We must predict target position to within ±14 μm at a distance at least 16 m from the gun barrel and 9 m from the nearest detector used for the prediction.[a] To provide adequate neutron shielding for any semiconductors in the target detection system, the detectors must stand back from the target injection path more than about 0.5 m.

The target speed is up to 400 m/s and injection rate is up to 6 Hz. The required injector accuracy of ±0.3 mrad and target diameter of 3 to 8 mm (nominally 4 mm) and detector locations all affect the required detector field of view.

The target tracking begins after a 2.5 m standoff from the gun barrel for sabot removal and target propellant gas removal.[b] This allows target velocity changes caused by propellant gas or sabot removal to be properly measured.

The simplified overall tracking system layout is shown in Fig. 1. Each detector shown consists of a pair of transverse position detectors (line scan cameras), two timing photodiodes that measure axial position and light sources for each sensor. The target position at chamber center (CC) is triangulated from positions at detector 1 (D1) and detector 2 (D2). The timing photodiodes are also used to trigger the transverse position detectors. The second timing photodiode signals at D1 and D2 will be used to predict target arrival at DCC. The time between this prediction and the signal from the second timing photodiode at DCC will be measured to determine the accuracy of the axial position prediction. The measurements from the DCC cameras will be used to correlate to the real-time predictions triangulated from the D1 and D2 measurements.

[a]The ±14 mm requirement allows a similar statistically independent error to be allotted to driver beam placement accuracy. The 9 m standoff distance includes about 6.5 m reaction chamber radius and 2.5 m of line of sight radiation shielding.

[b]Propellant gas is removed by expansion into a series of evacuated chambers separated by small openings for the target to pass through.

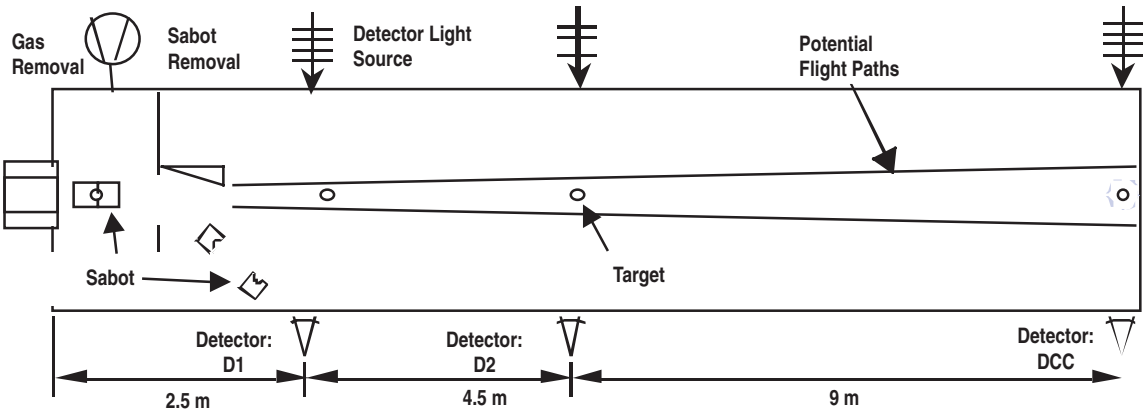

Fig. 1. Schematic of tracking system layout.

The required detector field of view (FOV) to see the entire target at any position that it is expected to pass the detector is given by

FOV = Gun accuracy x 2 x Distance from barrel + Max Target Diameter
= 0.0003 x 2 x Distance + 8 mm (for maximum diameter direct drive target)

- At D1, FOV = 9.5 mm
- At D2, FOV = 12.2 mm
- At DCC, FOV = 17.6 mm

The actual gun accuracy achieved to date has not met the ±0.3 mrad requirement. To track nearly all of the targets we have increased the FOV of D1 to 14 mm and are in the process of increasing the FOV for D2 and DCC to 40 mm. The equipment for the smaller (D1) and larger (DCC) FOV is shown in Fig. 2.

The size of the transverse position measurement errors allowed at the target detectors (D1, D2) that permit prediction of the final target position with the required accuracy is approximately ±2.3 μm.[1]

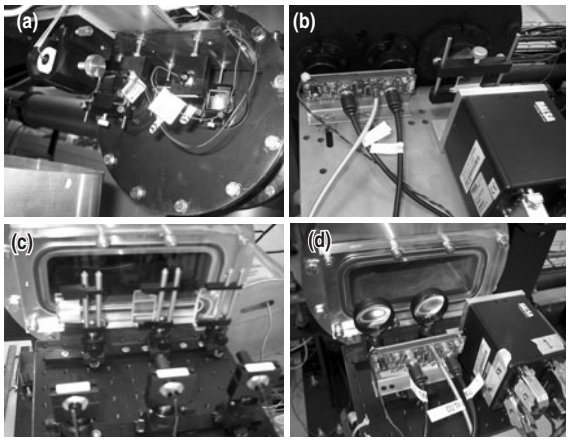

Fig. 2. (a,b) D1 Detector equipment with 14 mm FOV and (c,d) DCC detector equipment with 40 mm FOV.

III. TRANSVERSE DETECTION METHOD

A line scan camera is used for the transverse position detectors as illustrated in Fig. 3. The target is backlit with collimated laser light to produce as sharp a shadow as possible. The exposure time of the camera is set to view the target for ~1 μs as the center of the target passes.

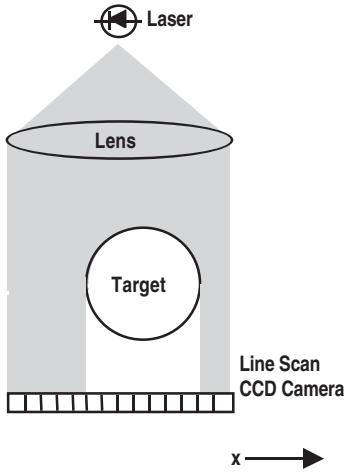

Fig. 3. Transverse target position is measured with a line scan camera. Target motion is into the page.

A pair of photodiodes triggers the line scan cameras. The diodes are positioned upstream of each camera a small distance so that the separation between the first diode and the second diode is the same as the separation between the second diode and the camera sensing element (80 mm separation). The shadow of the capsule passing the first photodiode generates a signal that triggers a counter to start the counter counting up. The

signal from the second photodiode switches the counter to counting down. When the counter reaches zero, a signal is sent to the line scan cameras to begin exposure.

We calculate the shadow center by finding the edges of the target shadow and taking the complement of the detector pixel's output and summing them according to

$$X = \frac{\sum_{i=min}^{max} iI_i}{\sum_{i=min}^{max} I_i} , \quad (1)$$

where i is the pixel number, min and max are the shadow edges, and I_i is the pixels output complement. The predicted transverse position of the target at DCC is triangulated from calculated positions at D1 and D2, correcting for the effect of gravity.

IV. AXIAL POSITION/TIMING METHOD

The timing sensors for axial position measurements are long, thin, single-element photodiodes. The targets are backlit with collimated laser light. The shadow of the target generates a current signal from the photodiode. This is fed into a current to voltage converter. The time that the output voltage drops below and rises above a reference value are precisely recorded by a time to digital converter. The midpoint time is used as the time that the target passed the timing detector. The time that the target passes the first two timing detectors is used to calculate the time that it will pass the DCC timing detector. The timing prediction signal flow path is shown in Fig. 4.

There are two digital delay generators. The first digital delay generator is preset to produce a delay signal out, after it is triggered, that is about half the flight time between D2 and DCC (~11 ms for 400 m/s). A preliminary signal starts the time to digital converter's time measurement. The falling signal from the D2 timing photodiode is sent to two places simultaneously. The first is for channel 5 of the time to digital converter. The second is the start trigger for the first digital delay generator. The CPU reads the time taken for the target to travel from D1 to D2, multiplies by the distance ratio of

$$(D2\text{-}DCC)/(D1\text{-}D2) = 2 , \quad (2)$$

makes corrections for the time between the rising and falling signals, then subtracts the preset delay put into the first digital delay generator. This quantity is then programmed into the second digital delay generator as the delay to be used when it receives its trigger from the first digital delay generator. This must be done in real-time as the target is flying from D2 to DCC.

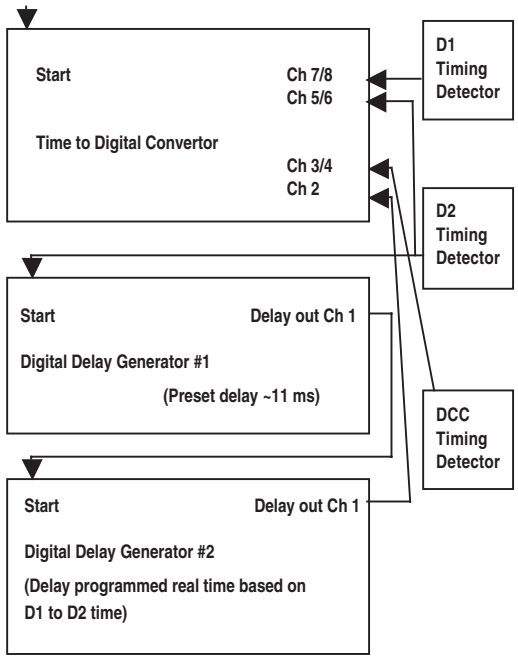

Fig. 4. Timing prediction signal flow path.

The timing photodiode at DCC triggers channels 3 and 4 of the time to digital converter. These signals will be compared to the predicted time of arrival received from the second digital delay generator. Our time to digital converters and digital delay generators achieve sub-nanosecond accuracy and at 400 m/s the target only moves 0.4 μm/ns.

V. FABRICATION AND TESTING RESULTS

We mounted the target tracking laser, line-scan camera, and optics in a target position detector assembly and tested the tracking system with a stationary target. A three-axis translation stage was mounted onto the equipment to allow the target to be precisely located (Fig. 5). The target was moved to nine separate locations each separated by 1 mm. When the target was moved away and returned to the same location, the position measurement results were reproducible to ±2.5 μm. The position measurement results are not quite linear. Over the range of 8 mm in target position, the position error from a least squares fit straight line was ±31 μm. We performed additional tracking system testing over a range of 1 mm and found the position error from an end point fit straight line varied rapidly and was ±10 μm.

The line forming laser diodes that we use for target position detection are not very uniform across the beam (Fig. 6). Additionally, the position detection tests show

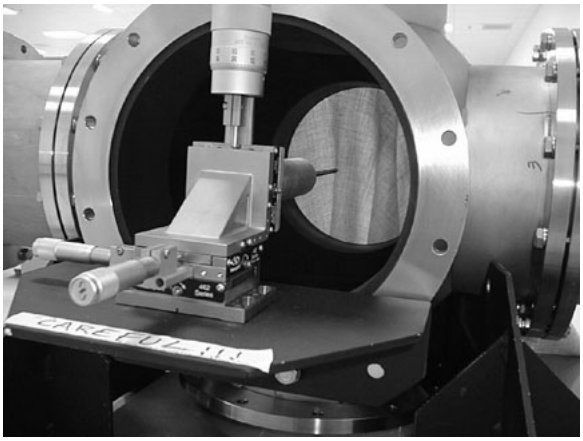

Fig. 5. Targets are mounted to translation stages for stationary tracking position measurements.

a significant amount of constructive and destructive interference of the laser illumination. The result is "ringing" at the edges of the target shadow.

We developed a QNX real time operating system driver for the Epix framegrabber and the Dalsa line scan camera. The driver allows the software to setup the camera to take an image and to store the image. We discovered that the Dalsa camera must operate at a minimum frame rate and modified the software to cause the camera to operate continuously prior to target arrival.

We setup the tracking assembly offline (Fig. 7) using air-rifle pellets and BB's for tracking projectiles. This off-line testing facilitated finding and correcting "bugs" in the tracking software. We brought the system operational with tracking tests up to about 300 m/s on each of the three detectors.

The tracking system has been operated with the full-scale injector and we now reliably achieve high-speed target position acquisition in one plane at the first target detector location (Fig. 6). The second two stations are in place, but are being modified (Fig. 2.) to increase the field of view to reliably track targets in flight (i.e. with the current placement accuracy). Timing detectors 2 and DCC were modified to trigger with a reduced threshold that is consistent with a larger field of view.

VI. IN-CHAMBER TRACKING

The tracking design described above measures target position and velocity outside of the reaction chamber and extrapolates the target position into the chamber. This requires either very low gas density or very consistent gas density and velocity in the chamber. We expect that actual chamber conditions will require additional target position measurements in the chamber. One method to achieve in-chamber tracking is an extension of our current design (Fig. 8). The standoff distance from the detectors will increase from 0.5 m to approximately 10 m. This will increase diffraction around the target and reduce the sharpness of the shadow on the camera. A narrow band optical filter is installed to keep chamber light off the detector. Mirrors and radiation shielding are installed to protect the light source, optical filter and camera. The mirrors should also be out of direct line of sight of the target explosion.

An alternative method for in-chamber tracking has been studied.[4] A stationary optical interference pattern is set up in the chamber (Fig. 9). Reflections of the interference pattern are sensed allowing measurement of the target position with accuracy of about 1% of the fringe separation. Interference patterns would be set up to provide a three dimensional grid within the chamber. The method can sense the targets relative position within a fringe, but not which fringe contains the target. External tracking is still needed to provide initial location data.

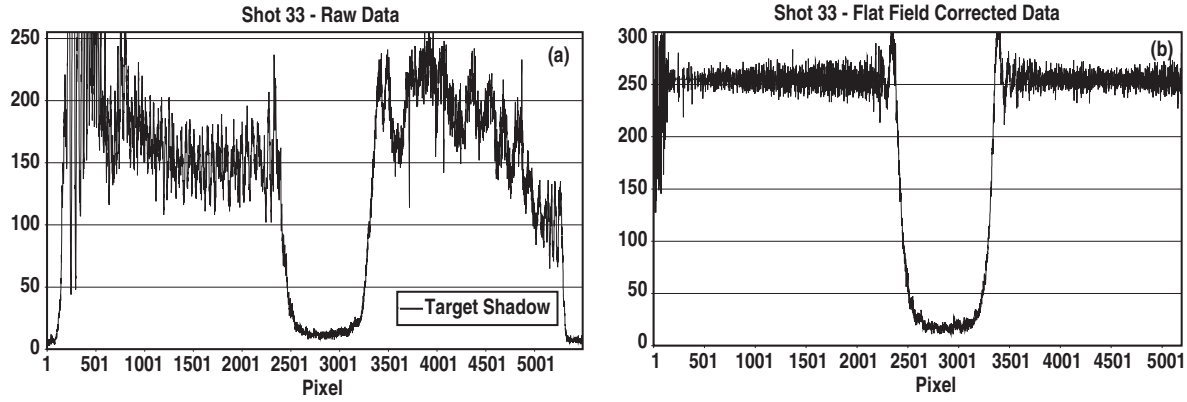

Fig. 6. Line scan camera image of target shadow from the first detector (a) raw data (b) flat field corrected data from the same shot. One pixel represents approximately 4 μm in the target plane. The flat field correction scales the raw exposure output data from each pixel by 255 divided by a value measured before the target arrival.

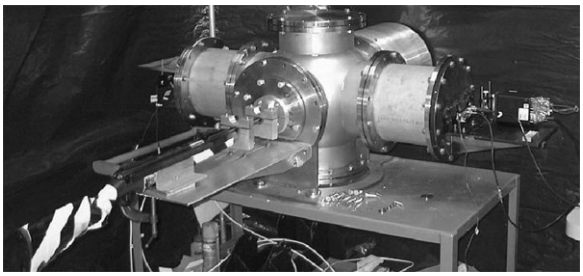

Fig. 7. Offline target tracking testing with air-rifle projectiles.

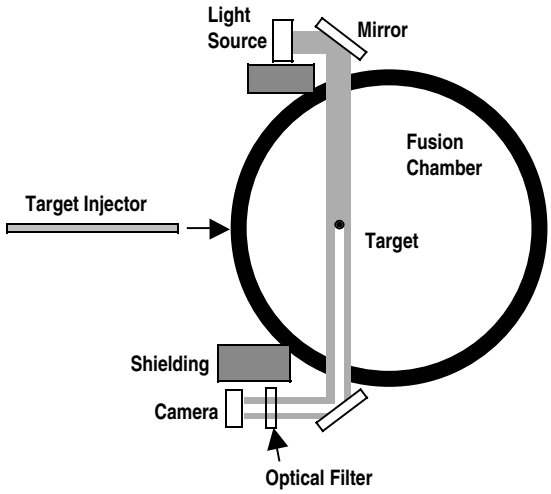

Fig. 8. In-chamber target tracking using a backlit target. The beam path is shown rotated by 90°.

VII. SUMMARY

The first phase (external from chamber) experimental target tracking and position prediction system has been designed. Components have been fabricated and installed for single axis tracking outside of the chamber. Modifications have been made for increased field of view measurements. Transverse position is measured primarily with line scan cameras. Position measurement repeatability of ±2.5 μm was achieved with stationary targets. Digital calculations will be performed to predict target transverse positions at chamber center based on these measurements. Targets are currently tracked in one plane at the first detector station only. Photodiode sensors detect the target arrival times. A time to digital converter and digital delay generators will be used to predict and verify target arrival times at DCC.

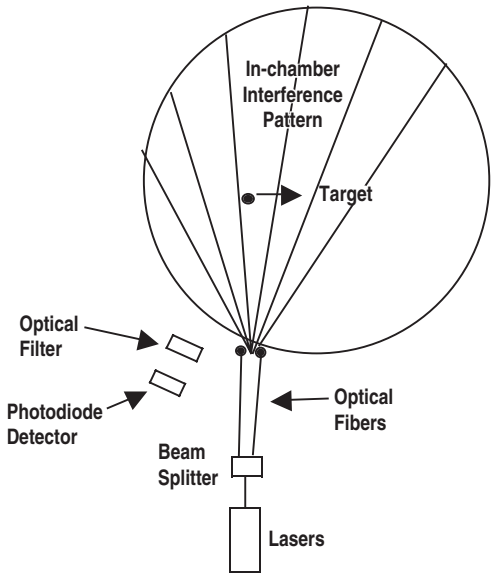

Fig. 9. Interferometric target tracking conceptual schematic diagram.

Tracking inside of the reaction chamber will probably be needed to measure changes in target position caused by chamber gas. Concepts for in-chamber tracking are being developed and evaluated.

ACKNOWLEDGMENT

This work was supported by the Naval Research Laboratory under Subcontract N00173-02-C-6010.

REFERENCES

[1] R.W. PETZOLDT, M. CHERRY, N.B ALEXANDER, D.T. GOODIN, G.E. BESENBRUCH, and K.R. SCHULTZ, "Design of an Inertial Fusion Energy Target Tracking and Position Prediction System," *Fusion Technology*, **39**, *No. 2* 678 (2001).

[2] J.D. SETHIAN, *et al.*, "Fusion Energy with Lasers, Direct Drive Targets, and Dry Wall Chambers," Nucl. Fusion **43** (2003) 1693.

[3] R.W. PETZOLDT, *et al.*, "Target Injection and Tracking System Design Requirements Basis," General Atomics Document 7-0001-02DR, San Diego, CA (2000).

[4] I. AGUROK, Phase II SBIR, DOE Contract DE-FG03-01ER83347, Physical Optics Corporation, Torrance, CA (2002-2004).